NEUROMECHANICAL CONTROL OF PADDLE JUGGLING

by

Avik De

A thesis submitted to The Johns Hopkins University in conformity with the requirements for the degree of Master of Science.

Baltimore, Maryland

May, 2010

Abstract

The objective of this research is to discover the rules by which the human nervous system controls the cyclic task of paddle juggling. The existence of separate feedforward and feedback control signals is hypothesized, and the feedforward control system is completely identified using tools from dynamical systems theory. Using this knowledge progress is made in identifying the feedback control system, with some interesting findings. The author believes that the data analysis methods in this work are novel and can be applied in the study of other hybrid dynamical cyclic tasks such as walking and running.

Primary Reader: Noah J. Cowan

Secondary Reader: Amy Bastian

Acknowledgments

The author would like to thank the Johns Hopkins Provost's Undergraduate Research Award for funding his research for the Summer of 2009. Apart from his advisor, he would like to thank Shai Revzen for fruitful conversations on phase estimation and Dr. Reza Shadmehr for his introduction to LTI subspace system ID.

Contents

Chapter 1

Introduction

1.1 The Neuromechanical System

The objective of this research is to discover the "rules" by which the human nervous system controls and adapts motor tasks that are of a cyclic nature (running, walking, juggling, breathing, etc.). For some of these tasks, especially in locomotion, it has been found that the dynamics of the mechanical system is critical to the the task [1, 2], and so we shall call the combination of the nervous system and the mechanical system dynamics the "neuromechanical" system.

While the mechanical system can be modeled reasonably using physics and physiology, there is no such easy way to model the nervous system. The brain is a "black box": we can only observe an output through some muscle activity corresponding to an input to the sensory systems. In the context of cyclic tasks, the "input–output"

notion turns into the idea of observing a response to a perturbation. A task such as walking is autonomous (not in the dynamical systems sense of the term), and there is a quasi-periodic output to no discernible input. Perturbations can cause deviations from a stable limit cycle, and following this the neuromechanical system attempts to return to the equilibrium orbit. The nature of the trajectory of this return exposes some of the characteristics of the closed-loop system.

The process of trying to understand the plant model from input–output data is generally termed as the system identification problem. As stated before, it is reasonable to assume that for many tasks, we can describe a "correct" model of the mechanical system using physics. Unfortunately, most of the time an accurate model would have a very large number of degrees of freedom and tunable parameters, and would be extremely complicated. A simpler model that has similar characteristics is often used instead [3, 4].

The validation of such a simplified model can still be complicated. This is because the mechanical system is in a closed loop with the brain, leading to issues of identifiability [5]. In the simplified block diagram of Figure 1.1, it is usually not possible to extract output data or inject input between the nervous and mechanical systems. As a result, we cannot tease apart the neural dynamics from the combined neuromechanical system dynamics by looking at only the input–output data. In fact, this difficulty motivates our choice of paddle juggling as the cyclic task of interest (see Section 1.3). Knowing the mechanical model exactly (we are assuming a fairly simple model for

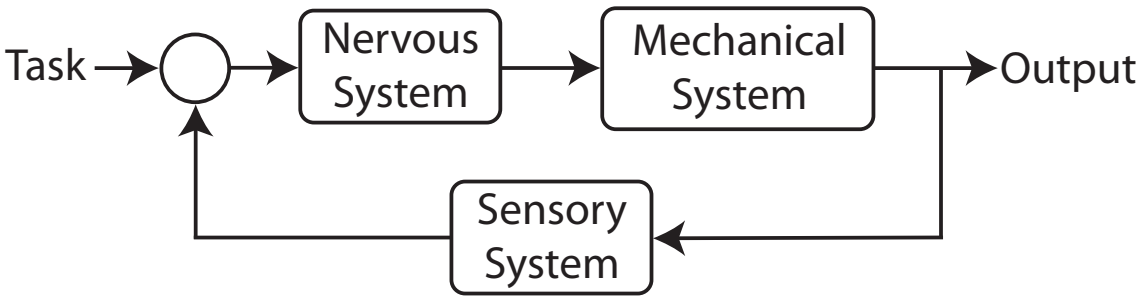

Figure 1.1: Simple model for neuromechanical control.

the muscle) makes it possible to learn what part the brain (controller) is playing in the closed-loop system by looking at input–output data.

1.2 Modeling as a Dynamical System

Walking, running and juggling are all examples of cyclic tasks, and we can consider the system output (for the case of juggling the output would include ball position and velocity, paddle position and velocity) to be generated by a hybrid dynamical system. We shall use the following representation for a hybrid system:

$$\Phi : \begin{cases} \dot{x} = f(x,u), \text{ where } u = \beta(\underline{y},t) \\ x \mapsto \pi_i(x), \text{ when } g_i(x) = 0 \\ y = h(x) \end{cases}$$

In the above equations, f represents the continuous time dynamics, h represents the output map, and the $\pi_i : \mathbb{R}^n \to \mathbb{R}^n$ are a finite set of state mappings that represent

the discrete "transition maps" in the terminology of [6]. In our case, the continuous dynamics include ball flight under gravity and a double integrator system for paddle movement. There is only one discrete transition, at the ball-paddle collision.

The function β is the control law, which uses a history of sensory inputs $\underline{y}$ for feedback,

$$\underline{y}(t) = \{\ y(\tau) : \tau \in (-\infty, t]\ \}$$

and also has a state–independent "feedforward" component which is made clear by the explicit time dependence. Section 2.1.1 has a detailed discussion of the feedforward and feedback parts of the control. The exact structure of β is not assumed to be known at this point; it may (for example) be the output of a dynamical system, or state feedback through a memoryless delay.

Note that for a cyclic system, f must be a nonlinear function in x. For the case of paddle juggling, Φ has a stable periodic limit cycle, $x^*(t)$. This means that

- when u is not state–dependent (no "feedback" component), $x^*(t)$ is invariant under the action of the state transition function f and the mappings π_i,
- $x^*(t+T) = x^*(t)$ for any t, where T is the "period" of the limit cycle.

1.3 Why Paddle Juggling?

We chose the paddle one-juggle as our cyclic task because the mechanical system is easier to model than for other tasks such as walking and running. The mechanical

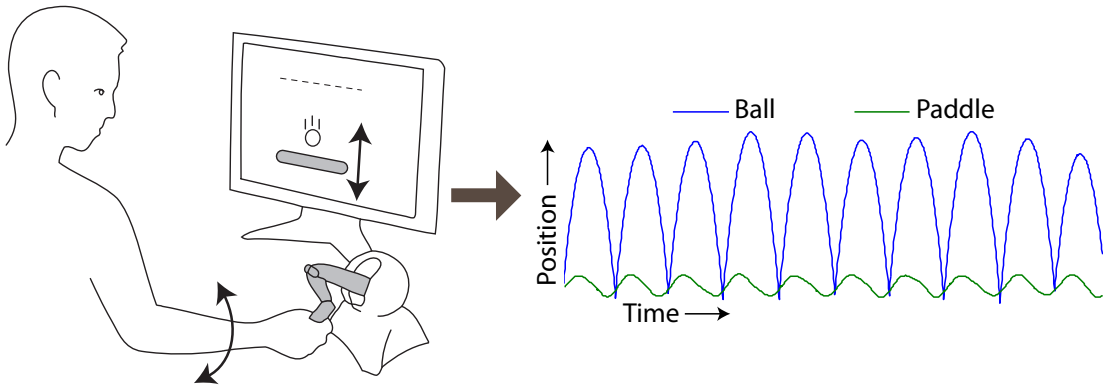

Figure 1.2: Experimental setup for paddle juggling. (Credit: Eatai Roth)

system needs only to include a model for paddle movement controlled by the arm. We may assume that the elbow exerts a torque, making the paddle dynamics a double integrator. The ball dynamics can be broken up into a continuous flight phase (constant gravitational acceleration), and a discrete impact step (non-elastic collision between the paddle and the ball). Simple physics can model this whole system, and all of the free parameters (paddle mass, ball mass, ball-paddle coefficient of restitution) are easily measured. The mechanical system model is formally written down in Section 2.2.

As discussed in Section 1.1, an exact knowledge of the mechanical system means that we have reduced our "unknowns" in the identification problem to just the neural dynamics. It is obviously difficult to formulate an exact mechanical model for a task such as walking, and this subsequently makes it difficult to extricate the neural dynamics from those of the mechanical system when dealing with input–output data.

Finally, it is easy to simulate the task in a virtual reality system, which enables us

to not only collect data easily, but also gives us the ability to perturb the physics in order to analyze the human response. This effectively means we can inject an input between the neural and mechanical blocks of Figure 1.1, using haptics to perturb the paddle downstream of the neural signal.

We used a "Stanford haptic paddle" [7] interface to a computer for data collection, eliminating the need for sophisticated data acquisition apparatus such as high speed cameras or motion capture equipment. For the experiments in this study, there was no haptic feedback to the user. Providing haptic feedback along with visual feedback (or some combination of the two) is among possible future work.

Chapter 2

Modeling

2.1 Feedforward and Feedback Signals

We hypothesize that the juggling control system has feedforward and feedback parts, whose constributions are summed to produce the input for the mechanical system. On the limit cycle, the feedback part is zero. However, small perturbations caused by noise or exogenous inputs excite the feedback component which tries to bring the system back to equilibrium. In the current work, we study the contribution of the feedforward input and visual feedback, and ignore slow changes to the feedforward input attributable to learning or adaptation.

To understand the distinction between feedforward and feedback input, consider the following conceptual experiment. A human subject performing closed–loop stable period one paddle juggling is suddenly blindfolded. The human will keep executing a

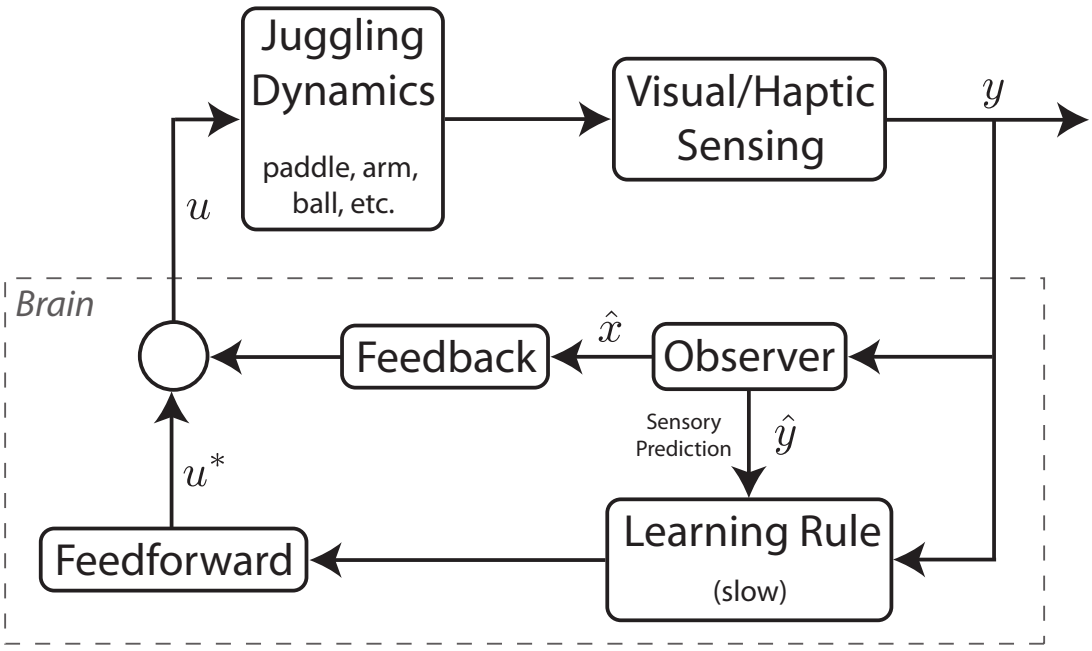

Figure 2.1: Detailed model for neuromechanical control of paddle juggling

"nominal" paddle trajectory which may or may not be stable—this nominal trajectory is the result of the feedforward control (because of blindfolding and neglecting haptic feedback, the feedback signal is zero). The visual feedback simply modifies this feedforward input in order to stabilize the ball–paddle system.

2.1.1 Feedforward vs. Nominal

It is worth noting that in a "black–box" system it might be impossible to perfectly distinguish feedforward control from a reflex based feedback control that is non–zero even at equlibrium (or on the limit cycle for a cyclic system). Consider the example of a mirror law paddle juggler [8], where the control law is purely feedback based.

The method discussed in this work would attempt to extract a "nomimal" paddle trajectory (the trajectory at the limit cycle) and fit a feeback control system which depends on perturbation of the state off the limit cycle. In most cases, a feedback augmented feedforward system may be equivalent in the input–output sense to the pure feedback system. However, as in the mirror law case, the pure feedback system may need fewer parameters and represent a more parsimonious description of the system. Further research is needed to devise a method which can truly separate the feedforward signal from a feedback signal.

In the present work, instead of trying to resolve this distinction we focus our attention on separating out a "nominal" trajectory and the feedback corrections to it. The control signal which generates the system output when the system is perfectly on the limit cycle shall be referred to as the nominal control input, and the trajectory generated by it the nominal trajectory. In the following chapters, we use the term "feedforward" interchangeably with "nominal". Consequently, the residual control signal when the nominal input is subtracted off is termed as the "feedback" signal. This terminology may not always be accurate, but as explained above, for our experimental setup (and for most practical purposes) the difference is imperceptible.

In subsequent sections we shall attempt to separate the feedforward and feedback control inputs from human data in order to compare their contributions in executing stable period–one paddle juggling.

2.2 Mechanical Model

Suppose the states of the mechanical system are written as x_1: ball position, $x_2 = \dot{x}_1$: ball velocity, x_3: paddle position and $x_4 = \dot{x}_3$: paddle velocity, and call

$$x_{(m)} = \begin{bmatrix} x_1 \\ x_2 \\ x_3 \\ x_4 \end{bmatrix}$$

the state vector (for only the mechanical system). The continuous dynamics follow the following equations:

$$\begin{aligned} \dot{x}_2 &= -\frac{g}{m_b} \\ \dot{x}_4 &= \frac{1}{m_p} u \end{aligned}$$

where m_b is the ball mass, m_p is the paddle mass, and $u(t)$ is the force input to the paddle exerted by torque at the elbow joint. In our simulation we used $m_b = m_p = 1$.

There is a discrete mapping of the states that happens at a ball-paddle collision. This collision happens when the following condition is satisfied:

$$x_1 - x_3 = 0 \text{ and } x_2 - x_4 < 0.$$

Let the collision map be defined as $x_i \longmapsto x_i^+$ for each state x_i. Then

$$\begin{aligned} x_1^+ &= x_1 \\ x_2^+ &= -\alpha x_2 + (1+\alpha)\, x_4 \\ x_3^+ &= x_3 \\ x_4^+ &= x_4 \end{aligned}$$

where α is the ball-paddle coefficient of restitution. The arm and paddle together are assumed to have sufficient inertia that the paddle velocity is not affected by the collision.

2.3 Sensing Model

We assume that the nervous system receives full knowledge of the four states considered above, with no added dynamics (i.e. no delay).

$$y = x_{(m)}.$$

For the present work we ignored haptic feedback.

Chapter 3

Feedforward Control System

Our first objective was to extract the "feedforward" (in the sense defined in Section 2.1.1) trajectory for period-one juggling from human trials. The simulated execution of a purely feedforward motion (Figure 3.1) to the juggling system will be referred to as "open-loop" paddle juggling. Our experimental setup was described in Section 1.3, and the number of trials we used was $N = 1$.

In future work, a priority is to incorporate multiple human trials in our experiment. The analysis provided in this thesis provides the theoretical basis for this future work.

It is an open question whether different individuals have the same feedforward "strategy" or if they use different strategies. In Figure 2.1 we explicitly included a block that slowly affected the feedforward strategy even for the same individual. (By "slow", we mean here over the scale of 10's or 100's of cycles). This can explain the effect of adaptation or "training" modifying the feedforward trajectory. Later in

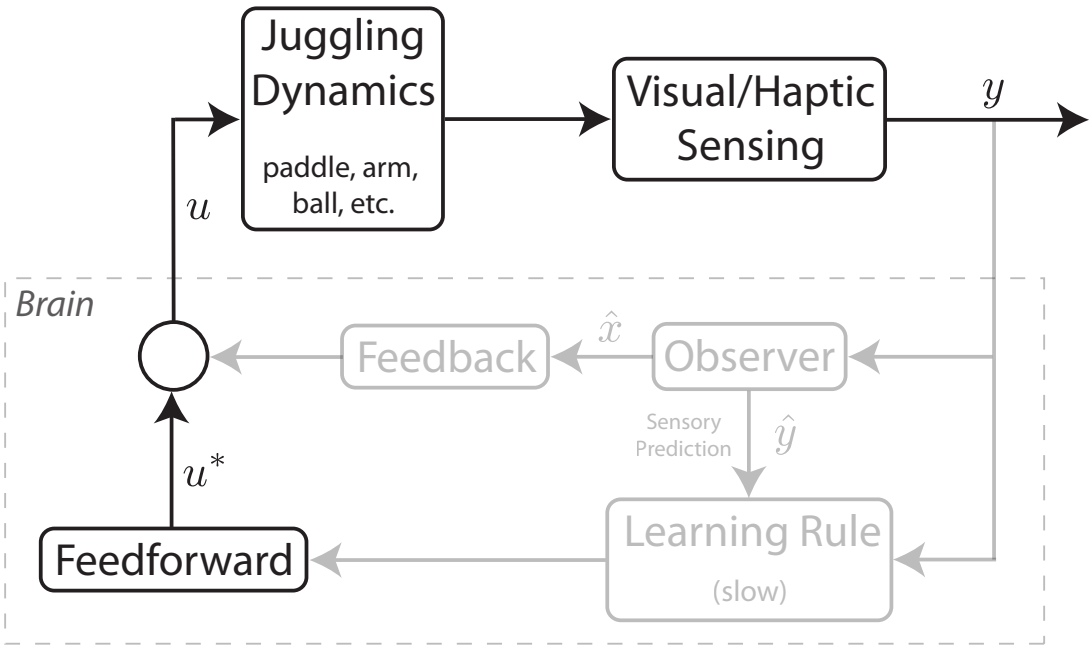

Figure 3.1: The block diagram for open-loop paddle juggling.

Chapter 4 we shall describe our hypothesis of a possible effect of adaptation in the feedback control.

3.1 Obtaining the Feedforward Trajectory from Data

We propose that the following experiment and data processing steps yield the feedforward trajectory. We collect data from a single individual executing period-1 paddle juggling *without perturbations* over a period of a large number (50-100) of

cycles. In the modeling step (Section 2.1) we stated that when the system is on the limit cycle, the contribution of feedback to the control input is zero. Since there are no perturbations, the only deviations from equilibrium occur because of noise.

First, we argue that the noise–induced deviations are zero mean in the original coordinate frame. If they were not, the human would likely "correct" for these deviations with a constant offset to the feedforward trajectory, so that the performance of the feedforward trajectory in the absence of sensory feedback is the best possible. In any case, a non–zero bias to the noise will be lumped into the feedforward trajectory we ultimately extract.

Secondly, note that for small deviations from equilibrium (it can be assumed that perturbations due to noise are small enough), the behavior of the nonlinear neuromechanical system can be described well by a linearization about the limit cycle. Hence the paddle trajectory (which is a system output) is related linearly to the noise input. Hence, it can be reasoned that by averaging the system output for a large number of cycles, we shall eliminate the contribution of the zero–mean noise, and what is left is the output caused by feedforward control.

3.1.1 Phase Extraction

Even though period-one paddle juggling is a periodic process (and we modeled it using a nonlinear system with a periodic orbit), in reality that data is *quasi-periodic*. Suppose that we can (by some unknown method) identify points in time when the

state of the system should be identical (exactly one time period apart), and these points are $\{t_1, t_2, \ldots\}$. Then it is not necessarily true that $t_{i+1} - t_i = T$ (the constant period of the system).

Instead of time, let us introduce an alternative notion called *phase*. Phase is an invertible mapping $\phi : \mathbb{R} \to \mathbb{R}$ such that $x(\phi_{i+1}) = x(\phi_i)$ on the limit cycle (using the shorthand $\phi_i = \phi(t_i)$ for brevity), and also $\phi_{i+1} - \phi_i = 2\pi$. So, while the time data $x(t)$ is quasi-periodic, the phase data $x(\phi)$ is strictly periodic with period 2π.

Note that often we use the term phase to refer to $\phi \bmod 2\pi \in S^1$, and the meaning should be clear from the context.

In this work, we have used the PHASER algorithm due to Revzen and Guckenheimer [9] for phase extraction from our time series data.

3.1.1.1 Change of Coordinates to Facilitate Phase Extraction

The method of Revzen and Guckenheimer was developed only for data which is an intrinsic mode function (IMF), meaning that the Hilbert transform of the time data winds around the origin at a rate strictly greater than zero. Paddle juggling data has discontinuities (for example, a phase space plot of ball position–ball velocity has a large jump in phase) which make phase extraction particularly difficult and unreliable.

We used the following nonlinear periodic change of coordinates in order to place the data in a coordinate frame more conducive to phase extraction. We show in

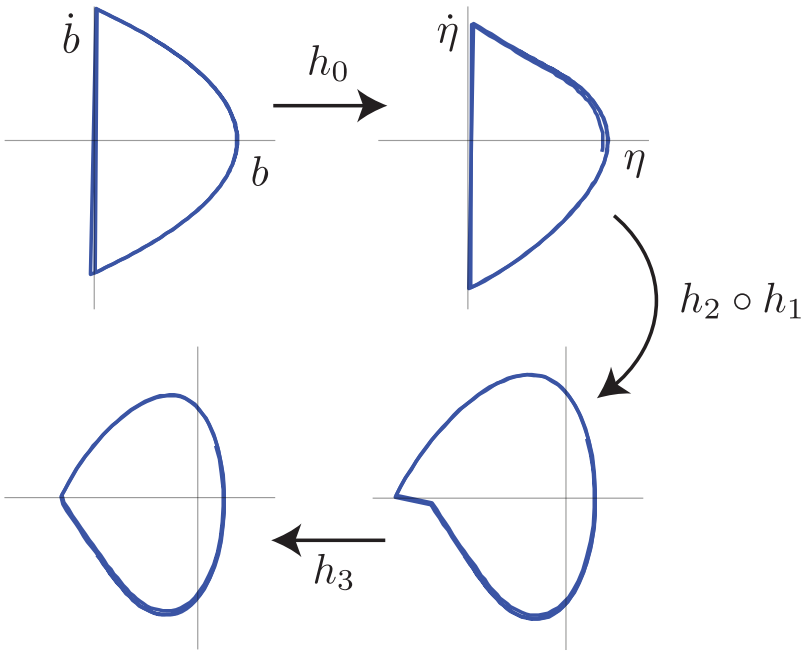

Figure 3.2: Nonlinear change of coordinates to remove phase discontinuities.

Appendix A that this does not affect the deterministic properties of the system (such as Floquet modes) that we seek to determine from our data.

Suppose the system output is $y \in \mathbb{R}^4$,

$$y = \begin{bmatrix} b \\ \dot{b} \\ r \\ \dot{r} \end{bmatrix}$$

where b is the ball position and r is the paddle position. Let $h_0 : \mathbb{R}^4 \to \mathbb{R}^4$ send

$$y \longmapsto \begin{bmatrix} b - r \\ \dot{b} - \dot{r} \\ r \\ \dot{r} \end{bmatrix} =: \begin{bmatrix} \eta \\ \dot{\eta} \\ r \\ \dot{r} \end{bmatrix}.$$

Note that h_0 is linear.

Let $h_1 : \mathbb{R}^4 \to \mathbb{R}^2 \times \mathbb{R}^+ \times [-\pi, \pi]$ convert $(\eta, \dot{\eta}) \mapsto (\rho, \theta)$ (from Cartesian to polar coordinates), while leaving $(r, \dot{r})$ unchanged. Because of physical constraints of the system ($b > r$ at all times), $\theta \in [-\pi, \pi]$.

Let $h_2 : \mathbb{R}^2 \times \mathbb{R}^+ \times [-\pi, \pi] \to \mathbb{R}^2 \times \mathbb{R}^+ \times S^1$ convert $\theta \mapsto 2\theta$, leaving everything else unchanged.

After the application of the change of coordinates

$$\begin{bmatrix} \rho \\ \theta' \\ r \\ \dot{r} \end{bmatrix} = h_2 \circ h_1 \circ h_0 \left(y \right),$$

note that output data on the limit cycle is still discontinous right at impact. This is because, after the collision,

$$\dot{\eta}^+ = -\alpha \dot{\eta}.$$

In order to compensate for this, we use the mapping $h_3 : \mathbb{R}^2 \times \mathbb{R}^+ \times S^1 \to$

$\mathbb{R}^2 \times \mathbb{R}^+ \times S^1$ that warps the ρ component via

$$\rho \longmapsto \rho \left(1 - \frac{\theta' + \pi}{2\pi} (1 - \alpha)\right).$$

Note that each of these transformations is invertible and smooth (the conversion to polar coordinates has a singularity at the origin, but that is safely avoided in real data since the empirically observed limit cycle is far from this set). To sum up, the transformation we apply to our juggling data is $h : \mathbb{R}^4 \to \mathbb{R}^4$

$$y \longmapsto h_1^{-1} \circ h_3 \circ h_2 \circ h_1 \circ h_0 (y).$$

The effect of these transformations in phase space is shown in Figure 3.2.

The method of [9] combines several scalar time series in order to give a more robust phase estimate. For paddle juggling we used the first and third components of y (after the change of coordinates above) for phase extraction. Note that the second and fourth components of y are simply derivatives of the first and third components, respectively. The Hilbert transform $\mathcal{H}$ (used to get protophases in [9]) has the property that

$$\frac{d}{dt}\mathcal{H}(x(t)) = \mathcal{H}(\dot{x}(t)),$$

so that adding derivatives of the scalar time series does not add any new information to the phase estimation process.

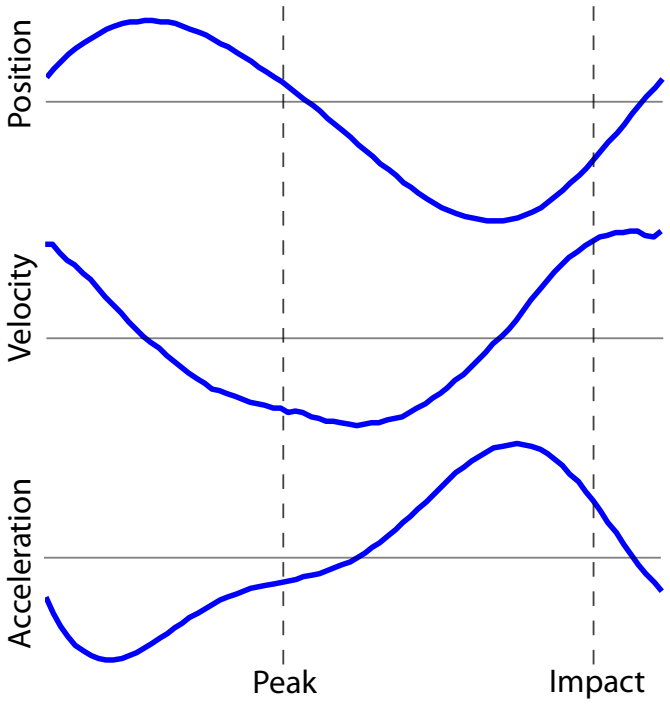

Figure 3.3: Nominal open-loop trajectory from human trial data.

3.1.2 Averaging to get Nominal (Feedforward) Trajectory

Suppose we call the collected output data $y_1, y_2, \ldots, y_p$. Once we have extracted the phase $\phi_1, \ldots, \phi_p$, we can average by binning in phase. For example, consider a division of the phase space

$$S^1 = \psi_1 \cup \psi_2 \cup \cdots \cup \psi_K$$

where the ψ_i are pairwise disjoint, and for any $\phi_i \in \psi_i$ and $\phi_{i+1} \in \psi_{i+1}$, $\phi_i < \phi_{i+1}$. Further, let $\rho_i = \{j \in 1, \ldots, p : \phi_j \in \psi_i\}$. The averaging is done in the following

manner:

$$\gamma_i = \frac{\sum_{j \in \rho_i} y_j}{|\rho_i|}.$$

The number of bins, K, controls the "resolution" of the average trajectory. If we have more data, we can afford to make K larger. In our trial, we used $K = 100$.

The data $\gamma_1, \ldots, \gamma_K$ is now the average trajectory. Figure 3.3 shows the nominal trajectory obtained by this method from our human trial.

3.2 Fitting a Model to Open-Loop Paddle Juggling

Since we know the exact feedforward trajectory of the human, we can now attempt to fit a model to open-loop paddle juggling (using the feedforward trajectory without feedback correction). As stated before, this system is periodic, nonlinear and time-varying. We shall attempt to find a model that explains only the linearized system (this will only be valid in the regime that linearization of the nonlinear system is valid, i.e. for small perturbations from the limit cycle).

Secondly, we shall also assume that the number of states in the system is known and is equal to 4 (same as the dimension of the output space). This assumption is related to the fact that the feedforward control system does not need an observer that would add additional dynamics and thus require more states.

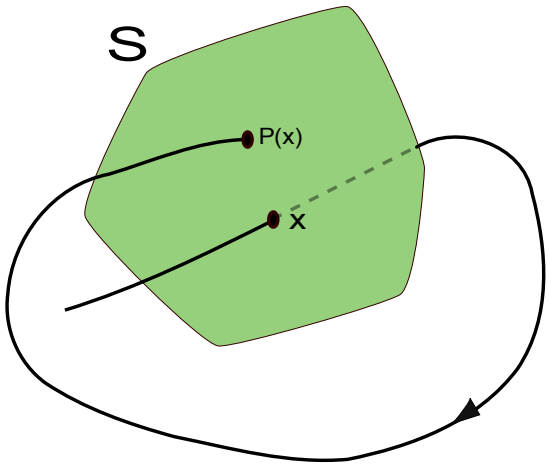

Figure 3.4: A Poincaré return map, where S is the codimension–1 manifold, and P is the return map. (Source: Wikipedia)

In order to extract the dynamics of the system, we did simulations with a ball bouncing on a paddle which is blindly executing the known feedforward trajectory. By simulating a rich assay of perturbations, we can excite all the dynamics of this system and then attempt to fit the input-output data. We need to use certain tools from dynamical systems theory in order to accomplish this from the simulated data, these are mentioned below.

3.2.1 Poincaré Return Maps

A Poincaré return map or first recurrence map (see Figure 3.4) is a useful tool in analyzing periodic systems. The map itself is the intersection of the orbit of the system with a lower dimensional section (usually of codimension 1) transverse to the flow of the system. This return map data is a discrete-time dynamical system in a

codimension 1 subspace of the ambient space, and it may be used to analyze some of the properties of the original system, such as stability.

Even though the theory of Poincaré return maps allows choosing any section transverse to the flow, there is a subtle issue with considering sections of constant phase as we have done in this work. When we are not on the limit cycle exactly, a particular section is not necessarily an *isochron* for trajectories ending up at the next section simultaneously. One may envision choosing sections in a special way so as to ensure that the time taken for the states to go from one section to the next is constant (as long as they are within a small cylinder around the limit cycle trajectory). This is a topic for future research.

3.2.2 Floquet Coordinates

Floquet coordinates are a coordinate frame in the ambient space of the dynamical system where the coordinate axes lie along the eigenvectors of the Poincaré return map. The main use of Floquet coordinates comes about as a result of Floquet's Theorem, which says that this coordinate change transforms the periodic system into a linear time invariant (LTI) system.

The procedure to find Floquet coordinates is similar to the procedure described in [10]:

1. Construct $M = 20$ sections of constant phase

$$\phi_i = \frac{i}{M} 2\pi, \ i \in \{0, 1, \ldots, M-1\}$$

and find the data at the sections by interpolating the phase data.

2. Find section maps $A_{i,j} \in \mathbb{R}^{4\times 4}$ by doing a least squares fit to section data. If $X_l = \{x \text{ at section } l\}$, then

$$X_i \ = \ A_{i,j} X_j \implies A_{i,j} = X_i X_j^{\dagger}.$$

We must take care to make sure that elements of X_i appear chronologically after (and within 1 period of) corresponding elements of X_j.

3. Pick an initial section, ϕ_k, and find the Poincaré return map for a section at ϕ_k. Suppose $X_k^{(0)}$ represents X_k with the last column removed, and $X_k^{(1)}$ represents X_k with the first column removed. Then a least squares fit for the return map matrix is

$$A_k = X_k^{(1)} \left(X_k^{(0)} \right)^{\dagger}.$$

4. Let $A_k = V_k D_k V_k^{-1}$ be an eigendecomposition of A_k. The Floquet coordinate axes at section k are the columns of V_k. Now these eigenvectors can be "propagated" using the section maps,

$$V_{k+1} = A_{k+1,k} V_k, \ V_{k+2} = A_{k+2,k+1} V_{k+1}, \text{ etc.}$$

Note that it must be true that $A_{k+2,k} = A_{k+2,k+1} A_{k+1,k}$, etc., however this is not a "constraint" enforced by our method of finding Floquet coordinates.

Tweaking this method to enforce this constraint should be considered a future avenue of research.

Let us denote the transformation to Floquet coordinates by $\mathcal{F}$. $\mathcal{F}$ is a periodic, time–varying, invertible transformation. Suppose the data obtained from the perturbation simulations mentioned in Section 3.2 is a time series $x_1, x_2, \ldots, x_p$, and we use the PHASER algorithm [9] to obtain the phase $\phi_1, \ldots, \phi_p$. Now we can convert the phase data to Floquet coordinates

$$x_k \xrightarrow{\mathcal{F}} z_k,$$

and by Floquet's Theorem, z_k are explained by an LTI system. Define $Z = [z_1, \cdots, z_p]$. Just like before we can fit

$$A_{\mathcal{F}} = Z^{(1)} \left(Z^{(0)}\right)^{\dagger}.$$

Now we can get back the phase varying system matrix $A(\phi)$, $A_{\mathcal{F}} \xrightarrow{\mathcal{F}^{-1}} A(\phi)$.

3.2.3 Open-Loop Stability

Now that we have a model for the open-loop system, we can examine its stability properties to see if feedback is necessary to stabilize paddle juggling. The acceleration curve in Figure 3.3 indicates that the acceleration of the paddle at impact time is positive. This suggests that the system is not passively stable [11].

To verify this "intuition", we did numerical simulations of open-loop juggling with time period ≈ 1 second starting from initial conditions very close to the limit cycle

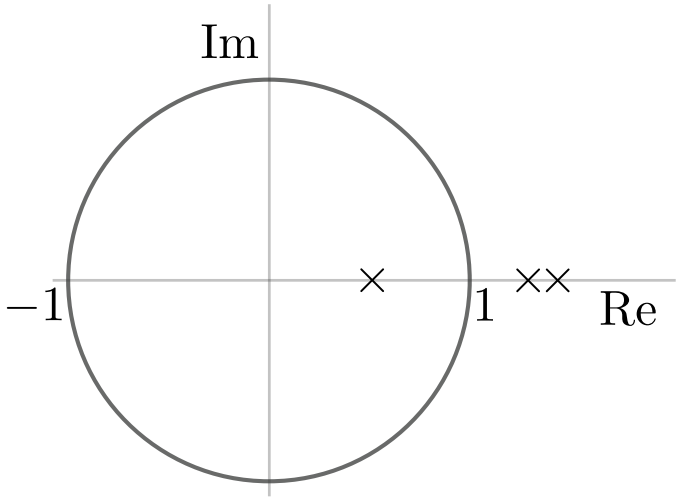

Figure 3.5: Eigenvalues of open-loop paddle juggling return map obtained from simulations.

(within the regime where the linearized system equations are valid. The resulting system has return map eigenvalues (see Section 3.2.1) that lie outside the unit circle (Figure 3.5), ergo the open-loop system is in fact unstable.

To sum up, human paddle juggling is not passively stable, and requires visual feedback for a time period of 1 second. There is a possibility that if the time period is reduced enough (so that visuomotor delays make visual feedback insufficient for feedback stabilization), the human switches to a trajectory that is passively stable. Experiments of this nature are part of future work.

3.3 Feedforward Trajectory as an Optimal Trajectory

Once we obtain the feedforward trajectory being used by the human (Section 3.1), a natural question to ask is why that particular trajectory was picked by the nervous system. We hypothesized that the trajectory used is the result of optimization of certain criteria like stability, performance and energy consumption. We can test these hypotheses by finding an optimal result satisfying the task constraints over the space of all trajectories, and then comparing this with the feedforward trajectory obtained previously.

3.3.1 Parameterizing Period-One Juggling Trajectories

For this section, we shall assume that the dynamics are continuous time. Suppose the paddle position is given by $x_p(t)$. Paddle physics is a simple double integrator, $\ddot{x}_p = u$. The constraints on the trajectory are

- $x_p(0) = x_p(T) = 0$ (can be set arbitrarily to any constant), and
- $\dot{x}_p(0) = \dot{x}_p(T) = V$, where V is the correct paddle velocity at impact to sustain ball flight of period T given the coefficient of restitution.

These differential constraints can be written as integral constraints on u after solving the linear system with a matrix exponential. This gives

$$\int_0^T u\left(t\right) dt \;\; = \;\; 0, \; \int_0^T tu\left(t\right) dt = VT.$$

We must first find a parameterization of the space of all trajectories. Since the trajectory is periodic, a natural choice is a finite order Fourier series:

$$u(t) = \sum_{k=0}^{Q} \left(a_k \cos\left(k\omega t\right) + b_k \sin\left(k\omega t\right)\right), \text{ where } \omega = \frac{2\pi}{T}.$$

Applying the integral constraints to this series results in a linear constraint of the coefficients,

$$\sum_{k=0}^{Q} \frac{b_k}{k} = -\omega V.$$

Because of this constraint, note that u can be specified by $2Q-1$ parameters, and that is the space of our optimization. In the next sections, we consider $u \in \mathbb{R}^{2Q-1}$.

3.3.2 Objective Functions

The objective function is a function $\text{OF} : \mathbb{R}^{2Q-1} \rightarrow \mathbb{R}$ that is minimized to get the optimal trajectory. We considered the following candidate objective functions:

1. **Minimum input.**

$$\text{OF}\left(u\right) = \int_0^T ||u\left(t\right)|| \, dt.$$

2. **Minimum jerk.**

$$\text{OF}\left(u\right) = \int_0^T ||\dot{u}\left(t\right)|| \, dt.$$

3. **Minimum goal error with white noise.** For this objective function we performed Monte-Carlo trials of the juggling system. Suppose $x_b(t)$ denotes the ball position. Then, at $t = 0$, $x_b(0) = x_p(0) = 0$ and define $V_b = \dot{x}_b(0) = gT/2$. This makes sure that $x_b(T) = 0$ and $\dot{x}_b(T) = -V_b$.

   Let $w(t) \sim N(0, \sigma^2)$ be i.i.d. noise. For $t \in [0, T]$, the paddle input affected by noise is

$$\tilde{u}(t) = u(t) + w(t).$$

   Note that this paddle trajectory noise will affect the impact time, and let the noise-affected impact time be called $\tilde{T} \neq T$. Suppose the paddle velocity on integration of the noisy trajectory gives $\tilde{V} = \dot{x}_p\left(\tilde{T}\right)$. The ball velocity after impact will be

$$\tilde{V}_b^+ = -\alpha V_b + (1+\alpha)\tilde{V}.$$

   The ball peak height after impact is

$$h = x_p\left(\tilde{T}\right) + \frac{\left(\tilde{V}_b^+\right)^2}{2g}.$$

   The objective function to minimize goal error is

$$\mathrm{OF}(u) = \sum_{\text{trials}} \left| h - \frac{V_b^2}{2g} \right|.$$

   We used $M = 1000$ Monte-Carlo trials for the optimization.

4. **Minimum goal error with signal-dependent noise.** Signal-dependent noise is a model studied and used widely in the neuroscience literature [12, 13].

This means that the motor control noise has a variance proportional to magnitude of the force exerted. For our model, the objective function is the same as in the previous case, except now

$$\tilde{u}(t) = u(t) + |u(t)|\, w(t).$$

In the steps above where we have used a norm $||\cdot||$ symbol, we tried optimization with both the 1-norm and the 2-norm. It is also worth noting that slightly different results may be expected from using $||u(t)||^2$ instead of $||u(t)||$ in the objective functions. The work in [14] reports that an exponent of $\approx$1.69 fits the data well for human reaching tasks.

3.3.3 Muscle Dynamics

For the minimum goal error objective functions, the best fit optimal model exhibited extreme (physiologically impossible) jerk. Keep in mind that the signal u is the output of the nervous system, and before this we have assumed that it is translated directly into elbow torque. However, the muscles actuating the elbow have their own dynamics which need to be modeled.

We have assumed that the muscle dynamics result in a low pass filter of the input signal. This assumption is based on the fact that any strictly proper rational transfer function (for a mechanical model of muscle) would exhibit low pass filtering properties. Furthermore, such models have gained traction in other similar modeling

studies [15]. In terms of the optimization mentioned above, high frequency neural signals get attenuated; this is effectively a truncation of higher order Fourier series terms in the elbow torque signal u.

3.3.4 Results

From our trials, **minimum goal error under signal-dependent noise** best matched our data by visual inspection. This is a nice validation of the applicability of a model used frequently in neuroscience [12] for the case of paddle juggling. The following caveats should be kept in mind:

- We only examined 4 different objective functions, whereas the brain may be optimizing a combination of these, or something entirely different. We based our choices on relevancy to physiology and the current neuroscience literature.

- A quantitative comparison of the trajectories to real data (over multiple cycles) will verify which model is the best. The procedure would be to fit the residuals from the model predictions to an ARMA process, and verifying that the residuals are mostly a stationary process.

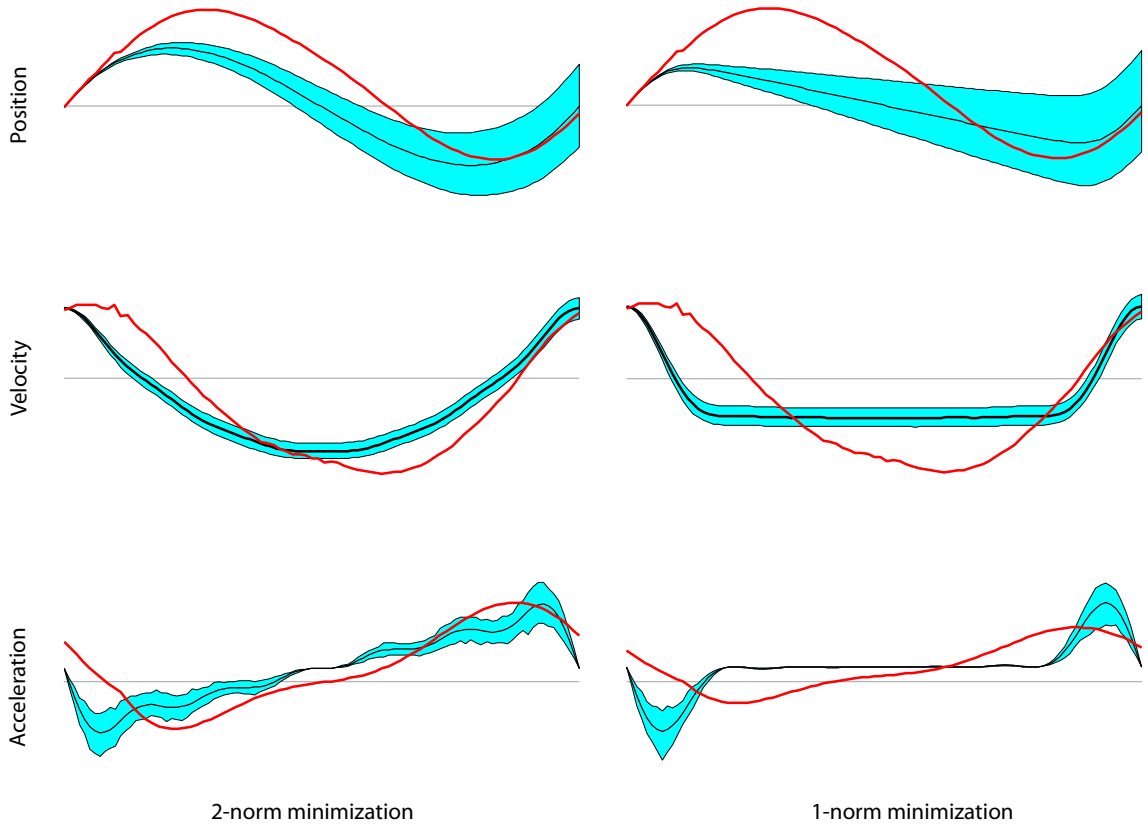

Figure 3.6: Minimum input. Note: for this plot and the subsequent optimization results, the x-axis is time from 0 to the juggling time period, and the y-axis is normalized to be the most visually accessible.

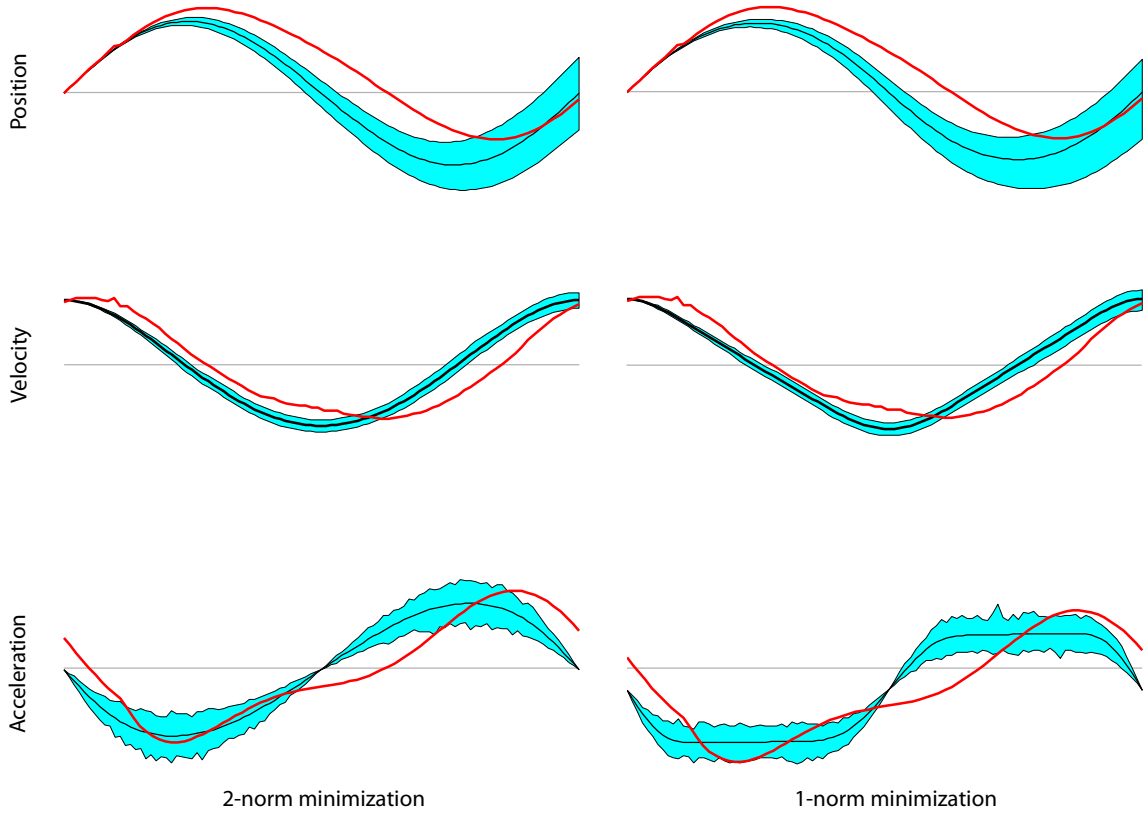

Figure 3.7: Minimum jerk.

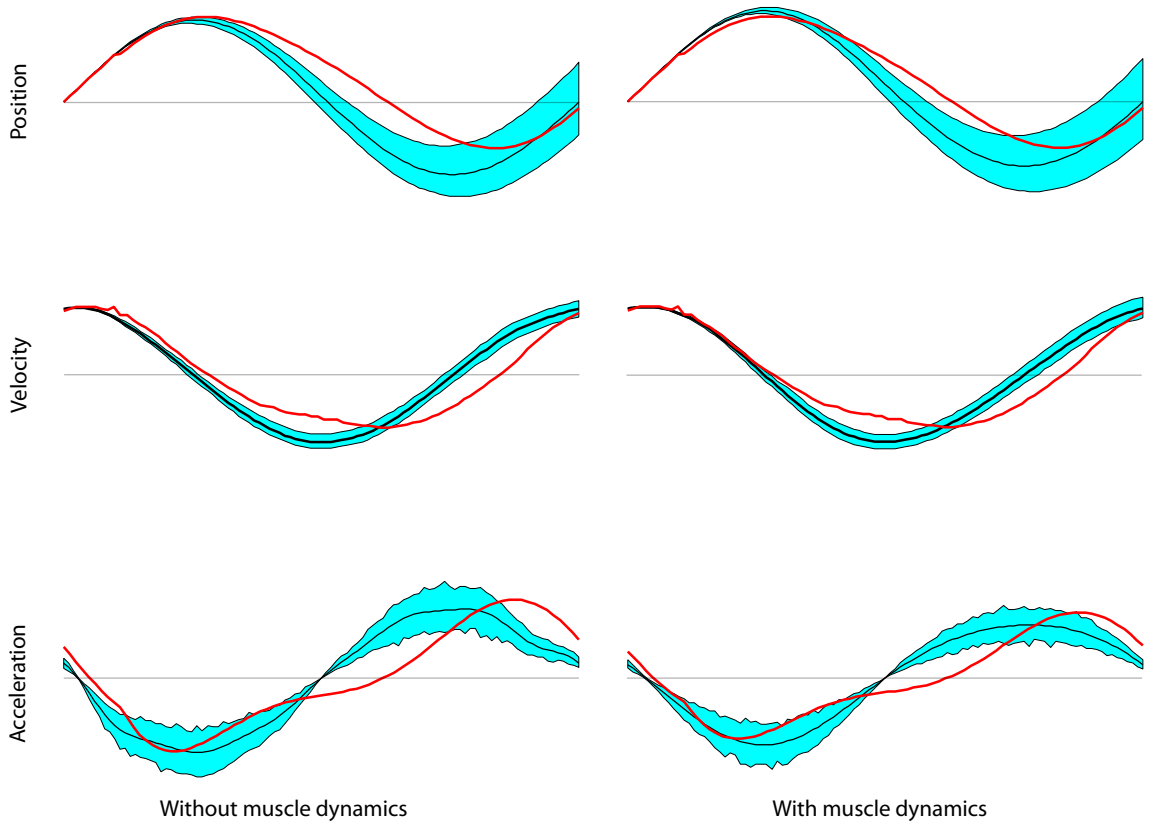

Figure 3.8: Minimum goal error with white noise.

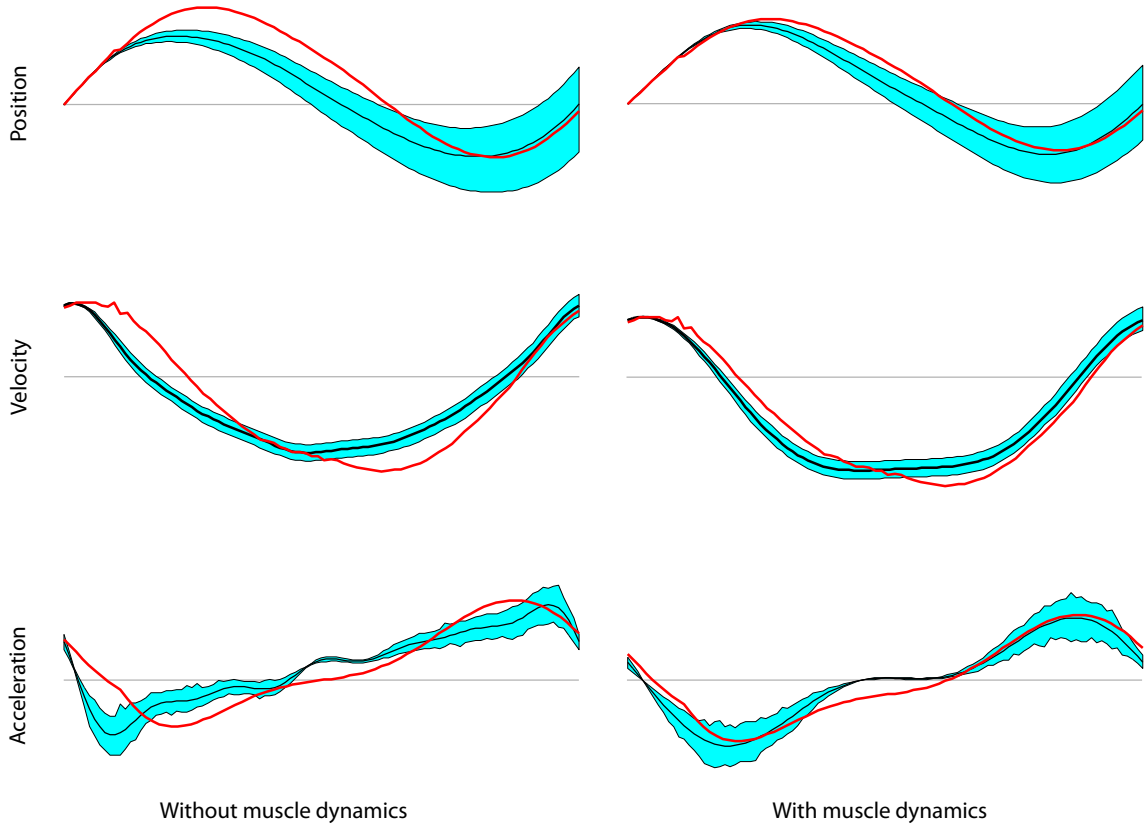

Figure 3.9: Minimum goal error with signal-dependent noise.

Chapter 4

The Role of Feedback

From the work in Chapter 3, we have a model for open-loop juggling (the result of feedforward control) in Figure 2.1. In order to establish models for the feedback control, we now include a feedback term that gets added to the feedforward signal (Figure 4.1).

The first question that needs to be asked is, how many states are in the neuromechanical system? This question is of fundamental importance, but is hard to answer from input-output data alone. In Section 3.2 we stated that it is reasonable to assume that the feedforward control system has no additional states, but a similar argument cannot be made for feedback control. Even for a simple linear system, a linear state observer doubles the number of states. In Section 4.2 we examine a structured way of answering this question.

Further, it is possible that there is a simple delay component in the feedback loop

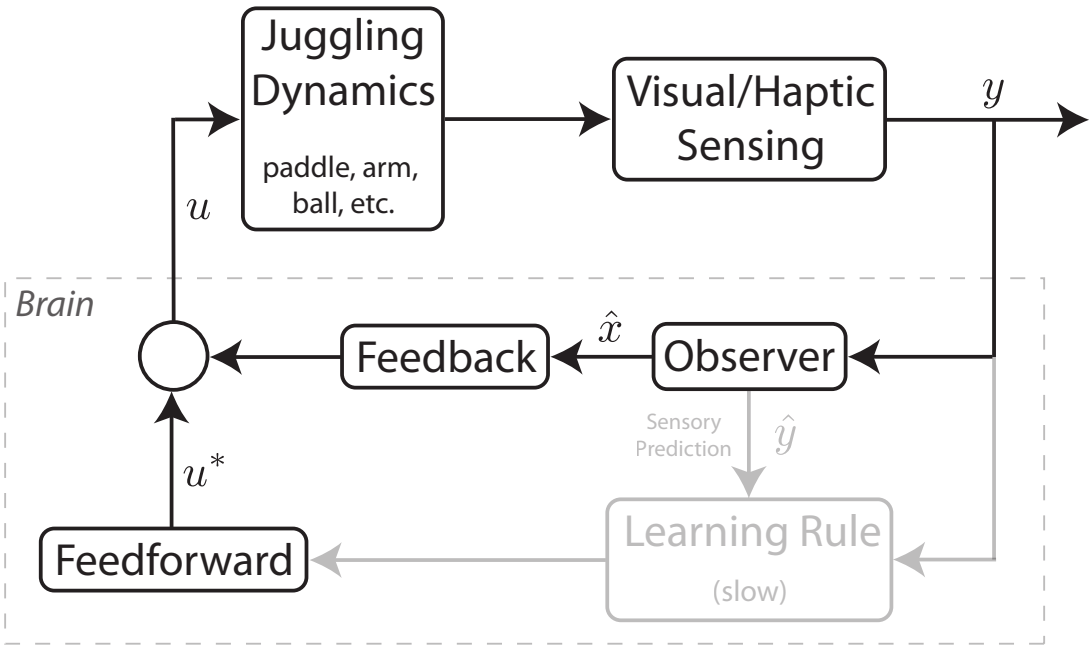

Figure 4.1: The block diagram for closed-loop paddle juggling.

because of the response time of the visuomotor system. Delays cannot be explained by finite state models and have to be accounted for separately.

The second question we asked is, when in the cycle does the human make the most use of visual feedback? We can assume that the human has full knowledge of the state of the paddle as a consequence of proprioception and an efference copy (cf. [16]), and the unknown states are of the ball only. The ball experiences free flight under gravity, and from simple physics it only takes two discrete observations of ball position to have full knowledge of its state. Intuitively, this means that the feedback signal should only need to make large corrections to the open-loop trajectory at a certain point in the

cycle. In Section 4.1 we show the results of a data-driven approach to answer to this question.

4.1 Magnitude of Feedback Signal

From our hypothesis of the structure of nervous control system in Figure 2.1, we stated that the feedback control input results in a correction to a feedforward trajectory for paddle juggling. In Section 3.2, we showed how to obtain a linearized phase-varying model of the feedforward control system, in discrete time. For this section, we shall write the same system in continuous time, for conceptual clarity.

Suppose $y(t)$ is a vector of the mechanical states of the system at time t; then the open-loop system evolves according to

$$\dot{y} = A_{\mathrm{OL}}(t)\, y$$

where the time varying nature of A_{OL} is made explicit. Note that it is periodic, so that $A_{\mathrm{OL}}(t+T) = A_{\mathrm{OL}}(t)$ for any t, where T is the period.

Then the closed-loop system evolves according to

$$\dot{y} = A_{\mathrm{OL}}(t)\, y + \mathrm{Feedback}(t)$$

where "Feedback" is the result, at time t, of the sumtotal of all the hidden dynamics in the feedback system affecting the observable states. It is a function of t and y, and the dependence of the latter is implicit in our notation. The important thing is that in this equation, the matrix $A_{\mathrm{OL}}(t)$ is known.

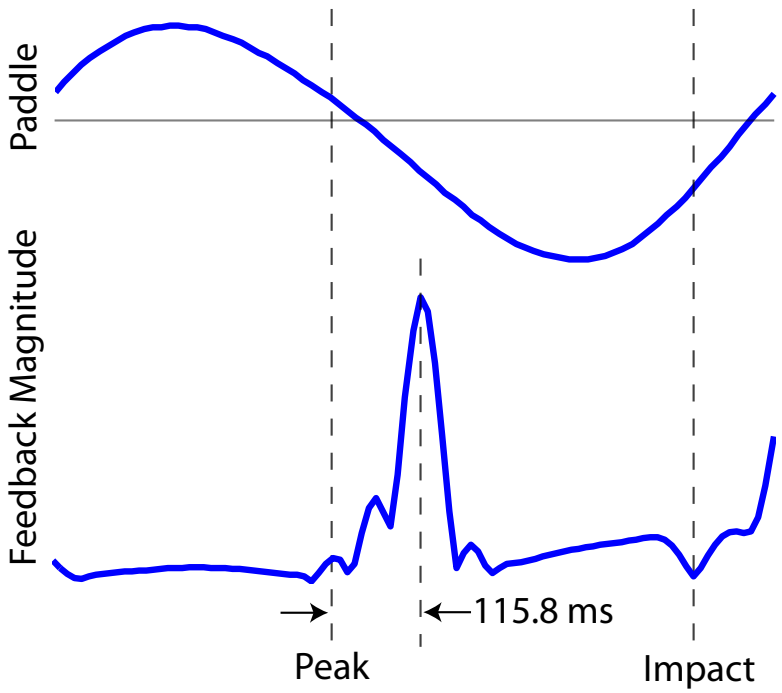

Figure 4.2: Plot of the magnitude of the feedback signal from pilot data along with the open-loop trajectory showing the large feedback input near the ball peak.

Using our experimental setup described in Section 1.3, we collected pilot data $y(t)$ of closed-loop paddle juggling. We propagated the mechanical state (measured at each time instant) through the open-loop model and compared this to the actual closed-loop data:

$$\text{FeedbackMagnitude}(t) = ||\dot{y}(t) - A_{\text{OL}}(t)\, y(t)||\,.$$

Resuts from our pilot data (shown in Figure 4.2) suggest that feedback is maximum 115.8 ms after the ball reaches the peak of its flight. This is just slightly shorter than visuomotor delays (≈150-250 ms, cf. [17]). This suggests that visual information during ascent right before peak is integrated to generate a stable estimate of apex state, which is sufficient for feedback control stabilization of the system.

This result gives us good insight on how to do structured perturbations of paddle juggling. For example, a perturbation of ball physics during ball ascent is likely to be corrected for in the same cycle, whereas a perturbation during ball descent may only be corrected for in the subsequent cycle.

Furthermore, the result also suggests that there is a delay component in the feedback loop, which should be accounted for in any detailed model of the feedback control system for and cyclic tasks that depend on visual feedback.

4.2 Subspace Analysis

Applying the Floquet method to the closed-loop system would assume knowledge of all the states, but the brain controller states are not readily available. The authors of [18] developed a method for state space system ID for LTI systems that uses the input–output data only and computes not only the dimensionality of the state space but also the system matrices themselves (up to a similarity transform). We developed an extension to their method to do system ID on linear parameter varying (LPV) systems.

Recently there have been other methods of subspace system ID developed such as in [19] where the authors compute the generalized observability matrix and determine the system matrices from there. On the other hand, our method (like the method of [18]) estimates the state sequence up to a change of coordinates, and then computes

the system matrices.

4.2.1 Problem Statement

In our juggling data, suppose we call the vector of hidden states of unknown size, x. Then the system equations can be written as

$$\begin{aligned} x_{k+1} &= A_{c(k)}x_k + Bu_k \\ y_k &= Cx_k \end{aligned}$$

where $c(k) = k - 1 \,(\mathrm{mod} K) + 1$, u_k is the exogenous input at instance k (this refers to, for example, a perturbation to the ball physics), and K is the period. The A matrix is periodic, but the B and C matrices are constant–meaning that the output map and the way the inputs affect the states do not change through the cycle.

4.2.2 Solution and Results

The solution method is demonstrated for a period-3 system in Appendix B, and the extension to other K is obvious and straight-forward.

This algorithm has been tested on simulated data of systems with $n = 3$ and $K = 3$. Its application to real juggling data is a part of future work.

Chapter 5

Discussion

In this work, we examine human paddle juggling as a simple example of neural control of a cyclic task. We demonstrate the usefulness of picking this particular problem by creating an experimental setup using a haptic paddle interfaced to a computer (Section 1.3). This system is easy to model, and we were able to collect pilot human trial data ($N = 1$ subjects). With this setup we can also perform systematic perturbation of the ball and/or paddle physics in real-time in order to observe the human response, in future work.

Our central idea is the existence of distinct feedforward and feedback control signals for generating paddle motions (Section 2.1). We hypothesize that the feedforward signal produces a periodic paddle trajectory that may or may not be stable, and the feedback part integrates sensory information (visual and haptic) in order to stabilize the mechanical states.

In Chapter 3, we set about trying to extract the feedforward trajectory from human data. We note that the data is not strictly periodic in time and introduce the concept of phase such that it is periodic in phase. We use an existing method for phase computation, and show how some additional data processing steps can make this phase estimation process easier (Section 3.1.1). In Section 3.2, we attempt to determine the characteristics of the open-loop dynamics with only the feedforward trajectory. We use the help of Floquet Theory to transform the data into a coordinate frame where the system is LTI and fit a linear system to it. This is a good model as long as we are "close enough" to the limit cycle that the linearized system equations are valid. We find that this open-loop system is actually locally unstable for a 1 second period paddle juggle by our single subject.

In Section 3.3 we evaluate a set of possible objective functions that the nervous system might be optimizing in order to "pick" the feedforward trajectory. This set of functions was chosen with particular attention to neuroscience literature, and our data suggests that the brain minimizes error in goal height assuming the existence signal-dependent motor noise, choosing optimal performance over energetic concerns.

Finally, in Chapter 4 we attempt to elucidate the nature of the feedback signal that corrects the feedforward trajectory from visual sensory information. In Section 4.1 we choose to not make assumptions about the structure of the system, but instead simply use our open-loop model from Section 3.2 to predict closed-loop data. The prediction error is exactly the feedback term. We showed that, averaged over many cycles, our

human subject injected a feedback signal whose magnitude peaked 115.8 ms after the ball peak. This indicates that the human uses the ball state information at and just before apex and makes corrections to the trajectory once per cycle. In Section 4.2 we show some progress in building a full-fledged system ID method for periodic linear state space systems, and envision that this method might be used to analyze closed-loop juggling data and fully understand the dynamics of the feedback "block".

With the intuition we have gained into neuromechanical control of paddle juggling, future work can delve deeper into making a good engineering model of the brain's contribution in controlling cyclic tasks (including separate feedforward or feedback signals). Also, the tools we have developed in this work can be applied to the analysis of other more complicated hybrid systems such as human walking, running or "real" (non paddle-) juggling.

Appendix A

Nonlinear Change of Coordinates

Consider an arbitrary discrete dynamical system

$$x_{k+1} = g\left(x_k\right)$$

with a fixed point $g\left(x^*\right) = x^*$. Now suppose we apply a nonlinear diffeomorphism h to get a change of coordinates $z_k = h\left(x_k\right)$, and define $z^* = h\left(x^*\right)$. Note that

$$z_{k+1} \;=\; h \circ g \circ h^{-1}\left(z_k\right),$$

and $h \circ g \circ h^{-1}\left(z^*\right) = z^*$. Now suppose we linearize z about z^*, and call $\Delta z_k = z_k - z^*$. Applying the chain rule for derivatives,

$$\begin{aligned}
\Delta z_{k+1} &= Dh|_{g\circ h^{-1}(z^*)} \cdot Dg|_{h^{-1}(z^*)} \cdot Dh^{-1}|_{z^*} \Delta z_k \\
&= \left(Dh|_{x^*} \cdot Dg|_{x^*} \cdot Dh^{-1}|_{z^*}\right) \Delta z_k.
\end{aligned}$$

Note that we can take derivatives of $h \circ h^{-1}(z^*) = z^*$ to get

$$\begin{aligned} Dh|_{x^*} \cdot Dh^{-1}|_{z^*} &= I \text{ (the identity transformation)} \\ Dh^{-1}|_{z^*} &= (Dh|_{x^*})^{-1}. \end{aligned}$$

Putting this in the previous equation, we get that

$$\Delta z_{k+1} = (Dh|_{x^*}) \cdot Dg|_{x^*} \cdot (Dh|_{x^*})^{-1} \Delta z_k.$$

This shows that the linearized z data and the linearized x data are both explained by systems that have the same eigenvalue structures, and are just a similarity transform away from each other.

Appendix B

Subspace LPV System ID

For the system model in Section 4.2.1, let $x \in \mathbb{R}^{n\times 1}$, $u \in \mathbb{R}^{p\times 1}$, $y \in \mathbb{R}^{q\times 1}$. Let i denote the "window size" (for our method the window size must be a multiple of the period). Let $j = r - 2i + 1$, where r is the number of data points. For the first

example, suppose

$$\underbrace{\begin{bmatrix} y_1 & y_2 & \\ y_2 & y_3 & \cdots \\ y_3 & y_4 & \end{bmatrix}}_{qi\times j} = \underbrace{\begin{bmatrix} C & C & C \\ CA_1 & CA_2 & CA_3 \\ CA_2A_1 & CA_3A_2 & CA_1A_3 \end{bmatrix}}_{qi\times ni} \cdot \underbrace{\begin{bmatrix} x_1 & & x_4 & & \\ & x_2 & & x_5 & \cdots \\ & & x_3 & & x_6 \end{bmatrix}}_{ni\times j}$$

$$+ \underbrace{\begin{bmatrix} 0 & & 0 & & 0 & \\ CB & 0 & CB & 0 & CB & 0 \\ CA_2B & CB & 0 & CA_3B & CB & 0 & CA_1B & CB & 0 \end{bmatrix}}_{qi\times piK} \cdot \underbrace{\begin{bmatrix} u_1 & & u_4 & \\ u_2 & & u_5 & \\ u_3 & & u_6 & \\ & u_2 & & \\ & u_3 & & \cdots \\ & u_4 & & \\ & & u_3 & \\ & & u_4 & \\ & & u_5 & \end{bmatrix}}_{pi^2\times j},$$

or, renaming matrices, $Y_{1|i} = \Gamma_i X_1 + H_i U_{1|i}$.

Similarly,

$$X_{i+1} = \underbrace{\begin{bmatrix} A_3A_2A_1 & & \\ & A_1A_3A_2 & \\ & & A_2A_1A_3 \end{bmatrix}}_{=\Theta_i} X_1 + \underbrace{\begin{bmatrix} A_3A_2B & A_3B & B & & & & & & \\ & & & A_1A_3B & A_1B & B & & & \\ & & & & & & A_2A_1B & A_2B & B \end{bmatrix}}_{=\Delta_i} U_{1|i}$$

For any matrices P and Q, define

$$P/Q = PQ^T \left(QQ^T\right)^\dagger Q$$

as the "projection" of the rows of P on to the rows of Q. Also define $Q^\perp$ as the space perpendicular to the row space of Q. Then $P/Q^\perp = P\left(I - Q^T\left(QQ^T\right)^\dagger Q\right)$, and $Q/Q^\perp = 0$. The idea is to eliminate the effect of U on Y by projecting onto a space perpendicular to U, so as to get a "linear" dependence of Y and X.

The system equations are

$$\begin{aligned} X_{i+1} &= \Theta_i X_1 + \Delta_i U_{1|i} \\ Y_{1|i} &= \Gamma_i X_1 + H_i U_{1|i}. \end{aligned}$$

From the second equation, $X_i = \Gamma_i^\dagger\left(Y_{1|i} - H_i U_{1|i}\right)$, meaning $X_{i+1} = \left(\Delta_i - \Theta_i\Gamma_i^\dagger H_i\right) U_{1|i} + \Theta_i\Gamma_i^\dagger Y_{1|i}$.

We can write,

$$X_{i+1} = \underbrace{\begin{bmatrix} \Delta_i - \Theta_i \Gamma_i^\dagger H_i & \Theta_i \Gamma_i^\dagger \end{bmatrix}}_{L_i} \underbrace{\begin{bmatrix} U_{1|i} \\ Y_{1|i} \end{bmatrix}}_{W_{1|i}}.$$

Now because we took $i = \mu K$ (some multiple of the period),

$$Y_{i+1|2i} = \Gamma_i X_{i+1} + H_i U_{i+1|2i} = \Gamma_i L_i W_{2|i} + H_i U_{i+1|2i}$$

Now we can try to eliminate the contribution of U to Y as follows:

$$\begin{aligned} Y_{i+1|2i}/U_{i+1|2i}^\perp &= \Gamma_i L_i W_{2|i}/U_{i+1|2i}^\perp + H_i \underbrace{U_{i+1|2i}/U_{i+1|2i}^\perp}_{=0} \\ \underbrace{\left(Y_{i+1|2i}/U_{i+1|2i}^\perp\right)\left(W_{2|i}/U_{i+1|2i}^\perp\right)^\dagger W_{1|i}}_{\triangleq O_{i+1}} &= \Gamma_i X_{i+1}. \end{aligned}$$

In the equation above, the left hand side is known, but the right hand side is unknown.We can get an initial factorization using SVD:

$$O_{i+1} = PSV = \underbrace{PS^{1/2}}_{E}\underbrace{S^{1/2}V}_{F}$$

As long as E and F have the right dimensions, we can always get the "correct" factorization by inserting a matrix T.

$$EF = (ET)\left(T^{-1}F\right)$$

We want $T^{-1}F = \hat{X}_{i+1}$. So

$$\underbrace{\begin{bmatrix} f_1 & f_2 & f_3 & \cdots \end{bmatrix}}_{F} = \underbrace{\begin{bmatrix} T_1 & T_2 & T_3 \end{bmatrix}}_{T} \underbrace{\begin{bmatrix} \hat{x}_4 & & & \\ & \hat{x}_5 & & \cdots \\ & & \hat{x}_6 & \end{bmatrix}}_{\hat{X}_{i+1}}$$

$$\begin{bmatrix} f_1 & f_4 & f_7 & \cdots \end{bmatrix} = T_1 \begin{bmatrix} \hat{x}_4 & \hat{x}_7 & \hat{x}_{10} & \cdots \end{bmatrix}, \text{ etc.}$$

The matrix on the left above must have rank n (use Sylvester's inequality to show this...). We can do another SVD to get a factorization of the form above to obtain T_1 and $\begin{bmatrix} \hat{x}_4 & \hat{x}_7 & \hat{x}_{10} & \cdots \end{bmatrix}$. In this way we can get $T = \begin{bmatrix} T_1 & T_2 & T_3 \end{bmatrix}$, and all the $\hat{x}_k$ (but $\hat{x}_4, \hat{x}_7, \ldots$ may be in different coordinates than $\hat{x}_5, \hat{x}_8, \ldots$).

To fix this, suppose we define

$$\bar{x}_k = P_{c(k)} \hat{x}_k,$$

and find P's such that the $\bar{x}$ are all in the same coordinates. Define

$$P_d = \begin{bmatrix} P_1 & & \\ & P_2 & \\ & & P_3 \end{bmatrix},$$

so that $\bar{X}_{i+1} = P_d \hat{X}_{i+1}$. So

$$O_{i+1} = EF = \left(ETP_d^{-1}\right) \bar{X}_{i+1}.$$

Now, we want ETP_d^{-1} to have the structure of Γ_i. In particular, the first "row"

must be $\begin{bmatrix} C & C & C \end{bmatrix}$. Suppose

$$ET = \left[\begin{array}{ccc|c} E_1 & E_2 & E_3 & \\ \hline & * & & \end{array}\right] \text{ (recall that } ET \text{is known)}$$

So now,

$$E_1 P_1^{-1} = E_2 P_2^{-1} = E_3 P_3^{-1}.$$

We can arbitrarily set $P_1 = I$ and get all the x's in the same coordinates as $\hat{x}_4, \hat{x}_7$, etc. After this step we have an estimate $\bar{X}_{i+1}$.

To obtain the system matrices, note that

$$\begin{bmatrix} \bar{x}_2 & \bar{x}_5 & \cdots \\ y_1 & y_4 & \cdots \end{bmatrix} = \begin{bmatrix} A_1 & B \\ C & 0 \end{bmatrix} \begin{bmatrix} \bar{x}_1 & \bar{x}_4 & \cdots \\ u_1 & u_4 & \cdots \end{bmatrix}.$$

We can backdivide to get the A_1, B, C matrices, and similarly all the other A matrices.

The Conditioning of Γ_i

$\Gamma_i^\dagger$ is well behaved when Γ_i is near square. If C has more columns than rows, we can redefine Γ_i with more rows in the following way:

$$\Gamma_i = \begin{bmatrix} C & C & C \\ CA_1 & CA_2 & CA_3 \\ CA_2A_1 & CA_3A_2 & CA_1A_3 \\ CA_3A_2A_1 & CA_1A_3A_2 & CA_2A_1A_3 \\ CA_1A_3A_2A_1 & CA_2A_1A_3A_2 & CA_3A_2A_1A_3 \\ CA_2A_1A_3A_2A_1 & CA_3A_2A_1A_3A_2 & CA_1A_3A_2A_1A_3 \end{bmatrix}.$$

This effectively means that $i = 6$ for the problem above, and some matrices such as the Y matrix need to be redefined. In the previous case, we had enough equations to solve for the matrices P, but in this case using $E_1P_1^{-1} = E_2P_2^{-1} = E_3P_3^{-1}$ only is not enough.

Just by counting, the matrix equation

$$\Gamma_i \begin{bmatrix} I_{2\times 2} & & \\ & P_2 & \\ & & P_3 \end{bmatrix} = ET \quad \text{(known } 6 \times 6\text{matrix)}$$

has 20 scalar variables and 36 equations for them. A simple nonlinear solver (such as the Levenberg-Marquardt algorithm in MATLAB) yields the correct solution.

Bibliography

[1] S. Collins, A. Ruina, R. Tedrake, and M. Wisse, "Efficient bipedal robots based on passive-dynamic walkers." *Science*, vol. 307, no. 5712, pp. 1082–5, Feb. 2005. [Online]. Available: http://dx.doi.org/10.1126/science.1107799

[2] N. J. Cowan and E. S. Fortune, "The critical role of locomotion mechanics in decoding sensory systems," *J. Neurosci.*, vol. 27, no. 5, pp. 1123–1128, 2007. [Online]. Available: http://dx.doi.org/10.1523/JNEUROSCI.4198-06.2007

[3] R. J. Full and D. E. Koditschek, "Templates and anchors: neuromechanical hypotheses of legged locomotion on land," *J. Exp. Biol.*, vol. 202, no. 23, pp. 3325–3332, 1999. [Online]. Available: http://jeb.biologists.org/cgi/content/abstract/202/23/3325

[4] J. Lee, S. N. Sponberg, O. Y. Loh, A. G. Lamperski, R. J. Full, and N. J. Cowan, "Templates and anchors for antenna-based wall following in cockroaches and robots," *IEEE Trans. Robot.*, vol. 24, no. 1, pp. 130–143, Feb. 2008. [Online]. Available: http://dx.doi.org/10.1109/TRO.2007.913981

BIBLIOGRAPHY

[5] S. G. Carver, T. Kiemel, N. J. Cowan, and J. J. Jeka, "Optimal motor control may mask sensory dynamics," *Biol. Cybern.*, vol. 101, no. 1, pp. 35–42, Jul. 2009. [Online]. Available: http://dx.doi.org/10.1007/s00422-009-0313-x

[6] P. Holmes, R. J. Full, D. Koditschek, and J. Guckenheimer, "The dynamics of legged locomotion: Models, analyses, and challenges," *SIAM Rev.*, vol. 48, no. 2, pp. 207–304, 2006. [Online]. Available: http://link.aip.org/link/?SIR/48/207/1

[7] C. Richard, A. M. Okamura, and M. R. Cutkosky, "Getting a feel for dynamics: Using haptic interface kits for teaching dynamics and controls," 1997. [Online]. Available: http://bdml.stanford.edu/DML/publications/richard2_asme97.pdf

[8] M. Bühler, D. E. Koditschek, and P. J. Kindlmann, "A simple juggling robot: Theory and experiment," in *Experimental Robotics*, 1989, pp. 35–73. [Online]. Available: http://www.springerlink.com/index/01337l1k72ntq571.pdf

[9] S. Revzen and J. M. Guckenheimer, "Estimating the phase of synchronized oscillators." *Phys Rev E Stat Nonlin Soft Matter Phys*, vol. 78, no. 5 Pt 1, p. 051907, 2008. [Online]. Available: http://www.biomedsearch.com/nih/Estimating-phase-synchronized-oscillators/19113155.html

[10] S. Revzen, "Neuromechanical control architectures of arthropod locomotion," Ph.D. dissertation, University of California, Berkeley, 2009.

[11] S. Schaal and C. G. Atkeson, "Open-loop stable control strategies for robot

juggling," in *IEEE ICRA*. piscataway, nj: ieee, 1993, pp. 913–918. [Online]. Available: http://www-clmc.usc.edu/publications/S/schaal-ICRA1993.pdf

[12] C. Harris and D. Wolpert, "Signal-dependent noise determines motor planning," *Nature*, vol. 394, Aug. 1998. [Online]. Available: http://www.nature.com/nature/journal/v394/n6695/abs/394780a0.html

[13] E. Todorov and M. I. Jordan, "Optimal feedback control as a theory of motor coordination," *Nature Neuroscience*, 2002. [Online]. Available: http://www.nature.com/neuro/journal/v5/n11/abs/nn963.html

[14] K. P. Körding and D. M. Wolpert, "The loss function of sensorimotor learning." *Proc Natl Acad Sci U S A*, vol. 101, no. 26, pp. 9839–9842, Jun. 2004. [Online]. Available: http://dx.doi.org/10.1073/pnas.0308394101

[15] D. B. Lockhart and L. H. Ting, "Optimal sensorimotor transformations for balance." *Nat Neurosci*, vol. 10, no. 10, pp. 1329–1336, Oct. 2007. [Online]. Available: http://dx.doi.org/10.1038/nn1986

[16] A. D. Kuo, "An optimal state estimation model of sensory integration in human postural balance." *J Neural Eng*, vol. 2, no. 3, pp. S235–S249, Sep. 2005. [Online]. Available: http://dx.doi.org/0/2/3/S07

[17] B. Mehta and S. Schaal, "Forward models in visuomotor control,"

Journal of Neurophysiology, pp. 942–953, 2002. [Online]. Available: http://jn.physiology.org/cgi/content/abstract/88/2/942

[18] P. Van Overschee and B. De Moor, *Subspace Identification for Linear Systems*. Kluwer Academic Publishers, Dordrecht, 1996.

[19] F. Felici, J.-W. van Wingerden, and M. Verhaegen, "Subspace identification of MIMO LPV systems using a periodic scheduling sequence," *Automatica*, vol. 43, no. 10, pp. 1684 – 1697, 2007. [Online]. Available: http://www.sciencedirect.com/science/article/B6V21-4PFDPMH-1/2/8b15e59a06e81f2806a5b9197dd6f4ed

Vita

Avik De started pursuing a B.S. in Mechanical Engineering at the Johns Hopkins University in Fall 2006. He will graduate in May 2010 with a concurrent B.S./M.S. degree from the Mechanical Engineering department (B.S. in Engineering Mechanics) as well as a B.S. degree in Applied Mathematics and Statistics. He was inducted into the Pi Tau Sigma honor society in 2008. He won the Robert George Gertsmeyer award in Mechanical Engineering (2009), the James Bell award for outstanding research in Mechanical Engineering (2010), the ASME award (2010) as well as an award for outstanding achievement in Applied Math (2010) from the Whiting School of Engineering. His research currently focuses on learning the mechanisms of neural control of cyclic tasks using dynamical systems theory. His previous research was on SLAM on graphs, on this subject he presented a paper for which he was the first author at the Workshop on the Algorithmic Foundations of Robotics, 2008. In Fall 2010, Avik

will start a Ph.D. program at the University of Pennsylvania under the supervision of Dr. Daniel E. Koditschek.